ELSEVIER

Ceramics International 30 (2004) 381–387

CERAMICS INTERNATIONAL

www.elsevier.com/locate/ceramint

Solid state sintering of red ceramics at lower temperatures

S.N. Monteiro, C.M.F. Vieira*

State University of the North Fluminense, UENF Advanced Materials Laboratory, LAMAV Av. Alberto Lamego, 2000, Campos dos Goytacazes, RJ, 28015-620, Brazil

Received 20 February 2003; received in revised form 8 May 2003; accepted 4 June 2003

Abstract

Red ceramic products based on clay minerals are normally fired above 900 °C. In practice, however, bricks have been produced at temperatures as low as 600 °C. In the present work the possibility of lower temperature solid state sintering of clay particles is theoretically explained based on geometrical aspects, vacancy diffusion and active surface bonding consolidation. A model of close-packed discs of a few micrometers in diameter and nanoscale thickness is proposed to explain a much more efficient sintering process for clay minerals than the classical spherical particle model. The proposed disc model presents specific characteristics of high contact surface area, lower porosity and nanoscale pores. The initial vacancy diffusion sintering rate is constant and several orders of magnitude greater than for the classical model. At 600 °C the completion of dehydroxylation in the clay crystals turns their flat surfaces into active sites for bonding consolidation.

Keywords: A. Sintering; A. Powders: solid state reaction; D. Clays; D. Traditional ceramics

1. Introduction

The final stage in clay ceramic processing, except for a few cases such as that of sun-dried adobe bricks, is a high temperature consolidation through firing. The scientific [1,2] and technological [3] literature on the sintering of red ceramics recommends temperatures above 900 °C. To our knowledge, the literature has never mentioned the possibility of firing clay ceramics, such as red bricks, at a temperature as low as 600 °C. In practice, however, this is indeed what happens in many brick industries in Brazil.

In the region of Campos dos Goytacazes, north of Rio de Janeiro, very fine and plastic clays [4] are used to make red bricks at firing temperatures no higher than 600 °C. These bricks surpass the minimum strength required by the norm [5]. Here the point is whether a lower temperature suffices to consolidate a red ceramic structure. The study of this possibility is the main purpose of the present paper.

2. Thermal behavior of clays

The specification of a proper firing temperature for red ceramics is a difficult scientific task due to the complex thermal behavior of a clay structure. Fig. 1 shows, as an example, a DTA curve of a typical kaolinitic clay from Campos dos Goytacazes. Temperatures above 400 °C are necessary for complete removal of the interlayer water [6]. An important reaction is dehydroxylation, which occurs in association with the endothermic peak from about 400 to 600 °C. During this reaction, the oxygen atoms become active sites for new bond formation [7].

Above 900 °C, glassy and liquid phases occurred due to the transformation of fine quartz particles and the presence of alkaline silicates [3]. The existence of fluid phases enhances the reaction kinetics and increases the chemical communication between the reacting phases [8]. Hence, temperatures, such as 900 °C [1] or 950 °C [2,3], are conventionally taken for granted as being the minimum for clay ceramic firing.

It is unquestionable that a higher level of temperature is convenient to consolidate a clay ceramic structure. However, clay particle union and porosity closing can also be achieved by pure solid state diffusion mechanisms. In fact, the classic solid state sintering process is

* Tel./fax: +55-22-27261533.
E-mail address: vieira@uenf.br (C.M.F. Vieira).

0272-8842/$30.00
doi:10.1016/S0272-8842(03)00120-2

able to explain the consolidation of unbonded particles into an almost fully dense body [9,10]. It will be shown in the present paper that the geometrical aspects of a clay mineral permit an efficient rate of structural consolidation at much lower temperatures than those conventionally accepted.

3. Effect of a clay particle size and shape

A typical particle of a clay mineral, such as kaolinite, is formed as a stack of double-sheet $6Al_2.Si_2O_5(OH)_4$ layers, with a flake or plate-shaped appearance. In the present paper we shall refer to a "clay particle" as the plate-shaped aluminum silicate crystal with a diameter less than 2 μm and nanoscale thickness. Well-crystallized kaolinite particles are composed of plates with hexagonal outline, while in poorly crystallized particles, this hexagonal shape is less distinct [6]. As shown schematically in Fig. 2, clay particles tend to be (a) hexagonal (well crystallized) or (b) disk-shaped (poorly crystallized). By contrast, [Fig. 2(c)], relatively large silicate particles, such as the ones found in silts, tend to exhibit a geometry comprising a round pile of plates stacked one on top of the other.

When moisture is added to an unburnt clay body, the water molecules fit in between the silicate sheets and form a thin film around the particles [1]. Plasticity develops in a mixture with sufficient water to satisfy both sheet coalescence and lubricating action [6]. Fig. 2 helps to understand that the smaller the particle, the larger its relative surface area and thus comparatively more water molecules could stick to it. Consequently, plastic bodies made with very fine clays are easily formed.

The influence of particle size on the characteristics of clay ceramics can be visualized using the Winkler diagram shown in Fig. 3. The shaded area, located in the center of the diagram, corresponds to the conventional field for red ceramic products. The region extending from the upper limit of the shaded area to the top corner associated with the clay fraction (<2 μm) corresponds to excessively plastic bodies. These are difficult to dry and could develop cracks after high temperature

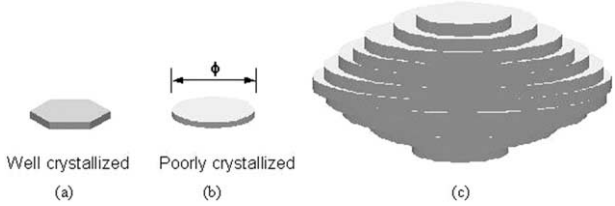

Fig. 2. Schematic size and morphology of aluminum silicate particles. (a) and (b) clay, $\phi < 2$ μm; (c) silt, $\phi > 2$ μm.

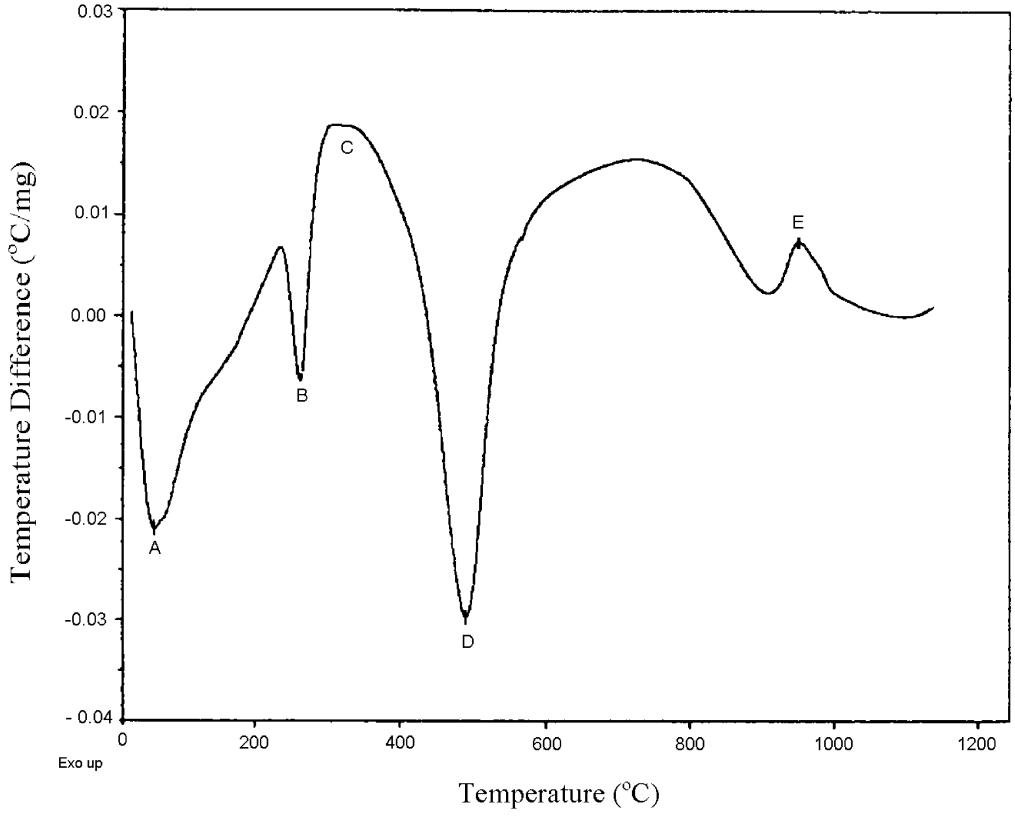

Fig. 1. Typical DTA curve of a kaolinitic clay from Campos dos Goytacazes showing peaks associate with: A = partial dehydration; B = decomposition of hydroxides; C = exotermic band of organic matter decomposition; D = dehydroxilation; E = formation of spinel from metakaolinite.

firing due to elevated shrinkage. Nevertheless, industries in Brazil are successfully using very plastic bodies, such as point **A** in Fig. 3, which is a typical clay extracted at Campos dos Goytacazes [4]. The reason for this successful use of a very plastic ceramic body is the relatively low firing temperature, less than 600 °C, applied in the fabrication of red bricks.

It will now be shown that a very plastic body, i.e., one that has a large amount of clay fraction such as **A** in Fig. 3, can be consolidated at temperatures lower than those conventionally used for red ceramic products.

4. Solid state sintering of aluminum silicate particles

4.1. The sphere model—relatively large particles

In classical sintering theory [9] the fundamental relationships that predict the rate of growth of the bonded area between particles are derived from a single model of equal spheres. The well known picture of two spheres developing a neck at the their contact point (Fig. 4), became the prototype of the initial stages of sintering. Several mechanisms can be used to explain neck formation based on the difference in free energy between the neck area and the surface of the particle [10]. If the vapor pressure is low, matter transfer by a solid state process occurs more readily. Out of six possible mechanisms only the transfer through the volume and/or from grain boundaries causes shrinkage and pore elimination, which typically happens in red ceramics. In this case the rate of bond formation between spherical particles, i.e., the solid state sintering rate [9] is given by:

$$x/t = \left(40\gamma a^3 D^* r^2/kTt^4\right)^{1/5} \quad (1)$$

where x is the radius of the contact area (“collar“ of the neck) formed between particles of radius r; γ the surface energy, D^* the self-diffusion coefficient, a^3 the atomic volume. Eq. (1) indicates that the sintering rate varies strongly with temperature, $x/t \propto T^5[\exp(-E_v/kT)]^{1/5}$, where E_v is the vacancy activation energy. At intermediate and low temperatures the sintering rate is comparatively lower. Furthermore, the sintering rate is roughly proportional to the inverse of the time, $x/t \propto 1/t^{4/5}$. Consequently, the velocity of neck expansion decreases with time and tends to zero for very large times.

One important parameter in the sphere model of Fig. 4 is the growth of neck expansion given by the ratio, x/r. According to Eq. (1), this ratio varies inversely with two-thirds power of the sphere radius, $x/r \propto 1/r^{2/3}$. Therefore, a very high sintering rate should be expected for particles in the nanosize scale, the so-called nanoparticles.

From a geometrical point of view the equal spheres solid sate sintering model is associated with specific conditions. Matter transfer between two particles has to start at a single contact point. The minimum initial porosity is 26%, which needs to be closed for full densification. In practical terms, for ceramic body behavior, the equal spheres model could be applied for the case of relatively large and round particle such as the one schematically shown in Fig. 2(c). This ceramic body would correspond, to the point **S**, located in the bottom area of the Winkler diagram in Fig. 3. The body **S** would have low plasticity and, from Eq. (1), would need high temperatures and demand longer sintering times.

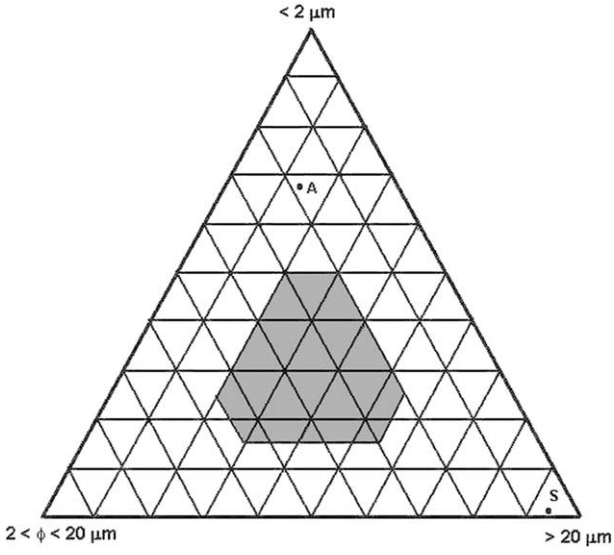

Fig. 3. Winkler diagram with corresponding gray field of red ceramic products.

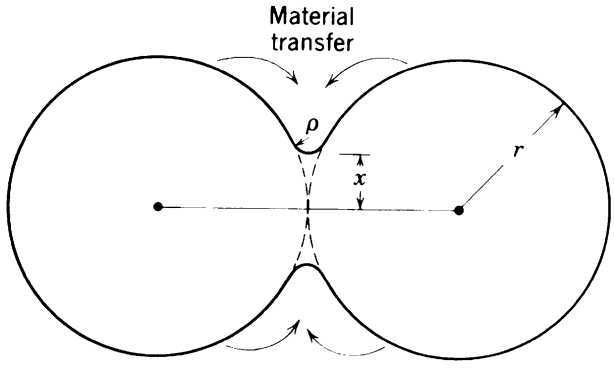

Fig. 4. Initial stage of sintering in an equal spheres model.

4.2. The disc model—clay particles

A realistic model for clay particles with sizes smaller than 2 μm is now proposed based on a disc-shaped geometry. This model is a better simulation for the solid state sintering of clay particles such as the ones schematically shown in Fig. 2(a) and (b). To simplify the model, it is assumed that a close-packed array of discs

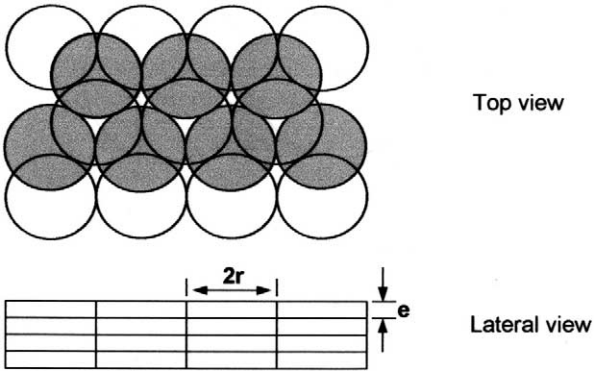

Fig. 5. Close-packed array of discs with ABAB stacking sequence.

with the same radius r and thickness e is stacked with their parallel flat faces in contact, as schematically shown in Fig. 5. The stacking sequence in Fig. 5 is ABAB, which means that in a top view, the discs in the third stack coincide with the ones in the first stack. The discs in the fourth coincide with the ones in the second stack, and so on.

Rather than discs the model could have used hexagonal plates, which are observed in small kaolinitic crystals [1,2]. But equal hexagonal plates, exactly like the one shown in Fig. 2(a), would then lead to the unrealistic possibility of a fully covered tridimensional space with perfectly matched particles. Here, the point is not to argue that clay particles could cover 100% of the space, which in theory is true. What we try to prove is that parallel disc-shaped particles are much more efficient for sintering consolidation than spheres. In fact, the close-packed array of Fig. 5, regardless of its stacking sequence, has a packing factor of 90.7%, which means only 9.3% of porosity. This is about one third of a close-packed array of spheres. As a consequence consolidation is easier to attain with discs than with spheres under the same solid state sintering conditions.

Another relevant characteristic is that a close-packed array of discs, such as the one in Fig. 5, as well as having contact points between discs in a same layer, also has contact areas between discs in adjacent layers.

In the model of Fig. 5, the area of contact for each disc is 92.5% of its own circular surface, both for ABAB stacking sequences shown in the figure and also for an ABCABC stacking. In both cases each disc is equally coupled with three discs in the lower and in the upper layers. Other possible close-packed arrays of discs are not as efficient for bond formation. For example, the AAA stacking sequence gives 100% of flat circular areas in contact but requires line bonding between cylindrical pile-ups of discs. This would correspond to an analogous sintering bond rate with neck growth as given by the sphere model in Fig. 4.

In a real situation one should not expect that an array of plate-shaped clay particles would be as perfect as the equal discs with the close-packed stacking sequence shown in Fig. 5. In nature the clay particles are neither perfect discs nor have the same size. However, when pressed together through a ceramic body forming operation, and after complete drying, a reasonably large area of contact between clay particles should be expected. Therefore, a simple geometrical model such as the one in Fig. 5 is sufficiently good to simulate and disclose the sintering ability of clay minerals.

5. Nanoscale solid state sintering of clay particles

As shown, a disc model (Fig. 5), has geometrical advantages for solid state sintering consolidation as compared to a sphere model (Fig. 4). However, the most important geometrical feature in the specific case of clay minerals is the nanoscale of the particle thickness. Although the clay particle diameter usually is not in the nanoscale, the sintering mechanisms are directly associated with their nanoscale thickness.

As far as solid state sintering is concerned, the remarkable advantage of nanoscale particles is that they may consolidate more readily than conventional particles [11]. The high specific surface area of nanoparticles provides an efficient driving force for consolidation. Furthermore, theoretical models [12,13] were proposed to predict the densification mechanisms during nanoparticle sintering. The models predict the possibility for closure of final nanoporosity. However, some differences from conventional sintering must be taken into account. The nanoparticle sintering simulation work of Zeng et al. [14] concluded that only two of the six classical mechanisms for matter transport during the initial stages are found to make a significant contribution for nanoscale sintering. These are surface diffusion and grain boundary diffusion, which are considerably accelerated by the large atomic forces near interfacial cusps.

The proposed disc model in Fig. 5 illustrates the importance of nanoscale mechanisms in the initial stages of clay particles sintering. Before examining the nanoscale mechanism it is worth reviewing the three geometrical features, which play an important role in the sintering of disc shape particles. These are:

- A relatively large contact area between the flat surfaces of the discs. If these contact surfaces become activated, then efficient bonding may be established.
- Micropores extending through the disc structure. In a sphere model, initially, there is only one network of open pores. In contrast, for each stacking sequence of a close-packed disc model there is a specific configuration of micropores.

For instance, the already mentioned AAA disc sequence has empty space running as an open channel or tubular micropore perpendicular to the disc plane. The ABCABC disc sequence has no micropores. In the specific ABAB sequence, used here to illustrate the proposed model, Fig. 5, half of the empty spaces between discs are tubular micropores. The initial solid state sintering of disc shaped clay particles micropores is similar to that of the sphere model, Fig. 4, where necks are formed at the discs tangent points.

- Nanopores corresponding to the empty spaces sandwiched between disc shaped clay particles. The convex triangular spaces, top view in Fig. 5, are nanopores with the same disc thickness. The other convex hexagonal empty spaces in Fig. 5 are tubular micropores. Nanopores do not exist in a closed-packed AAA disc sequence, whereas all empty spaces in an ABCABC sequence are nanopores of twice the disc thickness.

Once more it should be emphasized that in a real situation the clay particles in a pressed ceramic body will assume configurations much more complex than any of the mentioned close-packed disc-shaped sequences. In the same way that perfect spherical particles in a close-packed arrangement do not exist in practice. In spite of limitations in the sintering model of particles it is safe to affirm that pressed and dried clay ceramic bodies always have contact area, micropores and nanopores between particles. This results in the possibility of three separate sintering mechanisms, simultaneously, or otherwise, to take place.

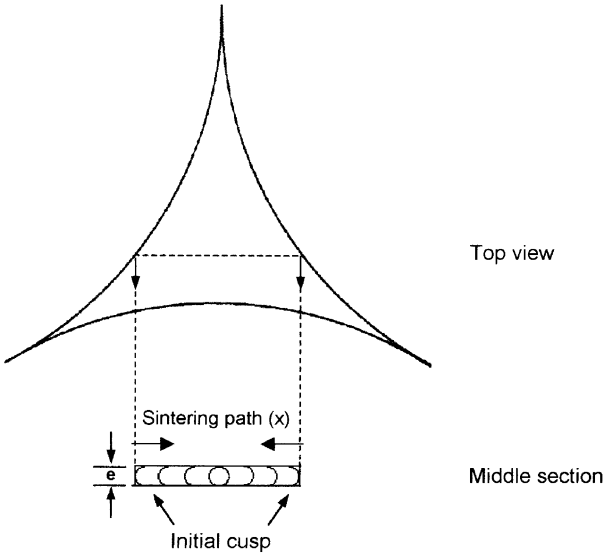

Fig. 6. Schematic view of nanopore from the disc model in Fig. 5 showing a middle section with suggested sintering path.

In particular, a nanoscale mechanism permits the initial sintering of clay particles to be many orders of magnitude more efficient than the conventional mechanism for spherical or common fiber shaped silicate particles.

6. Nanoscale sintering mechanism for clay particles

Clay particles with diameter less than 2 μm tend to be single crystals of nanoscale thickness, usually less than 0.1 μm. After the forming and drying operations on a clay ceramic body, its structure develops flat nanopores with about the same thickness as the particles themselves. Based on Zeng et al. [14], it is then assumed that the dominant sintering mechanism to consolidate the clay nonopores is surface diffusion.

Fig. 6 enlarges one of the nanopores of the disc model shown schematically in Fig. 5. A section across the thickness presents steps in the sintering front. It is assumed that the formation of a cusp or neck along the peripheral wall of the nanopore is the very first step. This cusp is formed by near surface diffusion of vacancies due to the difference in concentration between the cusp surface of high negative curvature and the flat surfaces [10]. The equation for the excess concentration of vacancies on the cusp with a radius of curvature equal to half of the thickness e is:

$$\Delta C = \left(2\gamma a^3/kTe\right)C_o \tag{2}$$

where C_o is the vacancy concentration on a plane surface and the other parameters have equivalent meaning as in Eq. (1).

Unlike the sphere model (Fig. 4), where the radius of curvature increases as the neck grows, the disc model (Fig. 6), maintains the same $\rho = e/2$ until the last step of the sintering path. In the perfect structure of the disc model of Fig. 5, the last step of the nanopore sintering path (Fig. 6), is the enclosing of transfer matter around a nanosphere with diameter equal to the disc thickness. This nanosphere is relatively stable with low surface energy.

The solid state sintering rate of the nanopore in Fig. 6 can be determined through the same classical derivation as for a sphere model [10]. The volume increment with time at the neck is given by:

$$dv/dt = J_v A/\delta \tag{3}$$

where J_v is the flux of vacancies, A the área of mass transfer, δ the density. Moreover, the flux of vacancies may be expressed by

$$J_v = \left(4D^* \Delta C\right)/a^3 C_o \tag{4}$$

Combining Eqs. (2), (3) and (4), the sintering rate or the speed of neck formation in Fig. 6 can be obtained

$$dx/dt = \frac{[8D_o \exp(-E_v/kT)\gamma]}{kTed} \quad (5)$$

For a given temperature this sintering rate is a constant. In the case of clay particles the rate may assume very large values due to its inverse relationship to their nanothickness. A simple comparison of the solid state sintering rates given by the sphere model, Eq. (1) and the disc model, Eq. (5), illustrates the enormous difference between them. As an exercise, we will assume possible values for the parameter in Eqs. (1) and (5) to compare the respective sintering rates. For the practical case of aluminum silicate, the specific values of D^*, a^3 and γ are not known but reasonable estimations could be:

- $D^* = 10^{-5}\exp(-60.000/T)$, from the work of Zeng et al. [15] in the sintering kinetics of α-Al_2O_3 powder.
- $a^3 = 10^{-30}$ m^3 for a cubic vacancy with 0.1 nm side.
- $\gamma = 1$ J / m^2, from Al_2O_3 system [10].
- $\delta = 3\times10^3$ kg / m^3.

Then, the calculated values for the sintering rates of both models with particle diameters of 2 μm, disc thickness of 0.1 μm, at 900 °C after 1 s are:

- sphere model; $x/t = 3.10^{-10}$ m/s.
- disc model; $x/t = 10^{-3}$ m/s.

Consequently, at conventional temperatures ordinarily used for firing red clay ceramics, and except for infinitesimal times, the sintering rate for nanopore is more than six orders of magnitude higher than the conventional consolidation model of spherical particles with same diameter.

It is also interesting to speculate on the efficiency of closing the nonopores of the disc model. If we assume that the displacement, x, of the front of matter transfer in Fig. 6 should be of the order of 1 μm for complete closure of the nonopore, then the time t required is approximately

$$t \cong 5.3T\exp(60\,000/T)10^{-27} \quad (6)$$

At 600 °C this time is about 10 h, which is of the order of the firing time used by the red brick industries in Campos dos Goytacazes. Now, if we try to calculate the time using the sphere model for the same $x = 1$ μm, only for a temperature of around 1000 °C is it possible to obtain a comparable time, i.e., 10 h. This implies that for round aluminum silicate particles such as the ceramic body **S** in Fig. 3, consolidation will first occur by liquid or glassy phase formation at 900 °C [1–3,6]. Only at 1000 °C or above, solid state sintering, according to the sphere model, becomes efficient for industrial production of aluminum silicate ceramic with relatively large, round particles.

7. Other sintering mechanisms for clay particles

The reasonable contact area between the flat surfaces of disc-shaped particles in Fig. 5 provides another bonding alternative for clay particles. Even if, in a natural clay mineral, this contact area is not as large as predicted by the disc model, it should be a relevant contribution to solid state sintering. For bonding between two surfaces of the same material to be achieved, either large compressive forces and high temperature are applied or the contact surfaces must be chemically activated. In the clay particles, however, a specific surface condition is observed. Normally the clay mineral has oriented water molecules tied to the surfaces of the particles through hydrogen bonds [6]. This serves not only in bonding the particles together but also facilitates the sliding between particles if a shear force operates. As long as water molecules cover the surfaces, no direct contact is able to occur between clay particles. Only above 60 °C (Fig. 1), one should expect dehydration to take place. In the case of kaolinite, solid state sintering by surface area contact is expected to begin above 400 °C where the complete dehydration and the activation of oxygen bonds associated with metakaolinite formation by dehydroxilation, should favor surface bonding between particles. Therefore it is suggested that an effective contribution to solid state sintering of clay particles by direct surface bonding should be attained at the end of the metakaolinite transformation, around 600 °C, in Fig. 1.

Complete dehydration of the surfaces is also a necessary condition for closing the nanopores formed by stacking clay particles according to the disc model of Fig. 5. Consequently, the mechanism proposed in the previous section based on Eq. (6) can only happen in a clay mineral at temperatures above 400 °C. Actually this is probably the minimum temperature that a clay ceramic body should be fired to permit, at least, partial consolidation to occur. However, if the data used for the practical estimation performed in this work are reasonable for clay minerals, then the time to close a nanopore at 400 °C exceeds one thousand years. For industrial interest the lower firing limit to consolidate red ceramics products would therefore be about 600 °C, according to our disc model.

The third possible solid state sintering mechanism for clay ceramic body consolidation is the closing of micropores like the channels with six convex sides shown in Fig. 5. This mechanism is analogous to the one proposed by the classical sphere model except for contact lines between stacks of discs rather than contact

points between spheres. The sintering rate for a micropore in a mechanically formed and dried clay ceramic body should not differ by more than one order of magnitude from that predicted by the classical model [9,10]. As already discussed, the solid state sintering consolidation of micropores in a close-packed stack of clay spherical particles should only be effective above 1000 °C.

Finally it is worth mentioning that the prediction of lower solid state sintering temperatures for the consolidation of clay particles of nanoscale thickness is in agreement with results for other materials [15,16]. Zeng et al. [15] found more than a 30% reduction in absolute temperature for sintering α-Al_2O_3 powders when going from 300 to 5 nm particle sizes. Livne et al. [16] studying the consolidation of nanoscale iron powder, indicated that it is possible to achieve high hardness on low temperature sintering. Another relevant point, which can be drawn from the disc model, is the general fact that nanoscale disc-shaped particles would require lower temperatures and would be much faster for consolidation by solid state sintering than spherical particles with corresponding diameter. But most important of all are the practical results obtained by the red brick industries, which have been successfully firing very plastic clay ceramic bodies at 600 °C. They contribute to cost saving, lower energy consumption and a cleaner environment.

8. Conclusions

A model for the solid state sintering of close-packed disc-shaped particles of nanoscale thickness was developed. The model simulates the consolidation mechanisms, which occur in very plastic ceramic bodies with fine clay particles (diameter <2 μm and thickness <0.1 μm).

Two specific geometrical features differentiate the proposed disc model from the classic sphere mode. First, the occurrence of nanopores of the same thickness as the disc-shaped particles. A sintering rate was derived for these nanopores and showed, for a given temperature, times many orders of magnitude lower than those predicted by the sphere model using realistic estimated values. Second, the existence of large contact areas between particles is implied. This is particularly efficient for the consolidation of clay ceramic bodies around 600 °C following complete dehydration and bonding activation by dehydroxilation of the clay mineral.

The estimated values for the sintering time obtained through the proposed disc model, corroborate the successful practice of producing red bricks from very plastic clay minerals, which were fired around 600 °C.

Acknowledgements

The support provided by the Brazilian Agencies: FAPERJ (process number E-26/151.544/2001), CNPq and FENORTE is gratefully acknowledged.

References

[1] W.D. Callister Jr., Materials Science and Engineering—An Introduction, 5th ed., John Wiley & Sons, New York, 2000.
[2] P.S. Santos, Science and Technology of Clays, 2nd ed., Edgard Blücher, São Paulo, Brazil, 1989 (in Portuguese).
[3] G.P. Emiliani, F. Corbara, Ceramic Technology, 1st ed., Gruppo Editoriale Faenza Editrice, Faenza, Italy, 1999 (in Italian).
[4] S.N. Monteiro, C.M.F. Vieira, Characterization of clays from Campos dos Goytacazes, north Rio de Janeiro State (Brazil), Tile & Brick Int. 18 (3) (2002) 152–157.
[5] Brazilian Association for Technical Norms, ABNT, Testing Method for Compressive Strength of Ceramic Blocks for Masonry, NBR 6461, Rio de Janeiro, June 1983 (in Portuguese).
[6] R.E. Grim, The clay mineral concept, Ceram. Bull. 44 (9) (1965) 687–692.
[7] G.W. Brindley, M. Nakahira, The kaolinite–mullite reactions series-1. A survey of outstanding problems, J. Am. Ceram. Soc. 42 (7) (1959) 311–324.
[8] M.P. Riccardi, B. Messiga, P. Duminuco, An approach to the dynamics of clay firing, Appl. Clay Sci. 15 (1999) 393–409.
[9] W.D. Kingery, M. Berg, Study of the initial stages of sintering solids by viscous flow, evaporation–condensation, and self-diffusion, J. Appl. Phys. 26 (10) (1955) 1205–1212.
[10] W.D. Kingery, H.K. Bowen, D.R. Uhlmann, Introduction to Ceramics, 2nd ed., Wiley-Interscience, New York, 1976.
[11] C. Suryanarayana, Nanocrystalline materials, Int. Mater. Rev. 40 (1995) 41–64.
[12] M.G. Mc Kimpson, Densification maps for nano-sized powders, Mater. Manufact. Process. 11 (6) (1996) 935–946.
[13] R.S. Iyer, S.M.L. Sastry, Consolidation of nanoparticles-development of a micromechanistic model, Acta Mater. 47 (10) (1999) 3079–3098.
[14] P. Zeng, S. Zajac, P.C. Clapp, J.A. Rifkin, Nanoparticle sintering simulations, Mater. Sci. Eng. A 252 (1998) 301–306.
[15] W. Zeng, L. Gao, L. Gu, J. Guo, Sintering kinects of α-Al_2O_3 powder, Ceram. Int. 25 (1999) 723–726.
[16] Z. Livne, A. Munitz, J.C. Rawers, R.J. Fields, Consolidation of nanoscale iron powders, Nano-Structured Mater. 10 (4) (1998) 503–522.